

Contents lists available at ScienceDirect

Case Studies in Nondestructive Testing and Evaluation

www.elsevier.com/locate/csndt

X-ray computed tomography for fast and non-destructive multiple pearl inspection

J. Rosc^a, V.M.F. Hammer^b, R. Brunner^{a,*}^a Materials Center Leoben Forschung GmbH, Roseggerstraße 12, 8700 Leoben, Austria^b Natural History Museum Vienna, Department of Mineralogy and Petrography, State Gem Institute, Burgring 7, 1010 Vienna, Austria

ARTICLE INFO

Article history:

Available online 29 August 2016

ABSTRACT

X-ray computed tomography displays a highly valuable nondestructive testing tool in various fields. A major disadvantage of this method comprises its high operating costs. Therefore, the reduction of the scanning times would be highly beneficial. Here, we demonstrate exemplarily for the testing of pearls the possibility to decrease the scanning times. The great diversity of pearls on the market, often of unclear origin, especially used for jewelry, demands non-destructive test methods for the fast and reliable classification and validation. We discuss the use of a nano-focus X-ray computed tomography (nf-XCT) system for fast three-dimensional characterization to distinguish between natural and cultured pearls. We test the approach not on individual pearls but for a more demanding task namely for a pearl necklace, that is multiple pearls on a strand. We show that with just one scan the 3D image data of the individual pearls within the whole necklace, which is composed of about 200 pearls can be scanned and reconstructed in only about 24 minutes. That is, we illustrate that nf-XCT as a inspection method is highly competitive to conventional radiography or radioscopy. The presented work also reveals possibilities for other fields like microelectronics etc.

© 2016 The Author(s). Published by Elsevier Ltd. This is an open access article under the CC BY-NC-ND license (<http://creativecommons.org/licenses/by-nc-nd/4.0/>).

1. Introduction

In recent years lab based X-ray computed tomography (XCT) has become an important nondestructive testing (NDT) tool in various fields like material science [1,2], bones and minerals [3,4], microelectronics [5,6] etc. The major advantage of XCT in comparison to other X-ray imaging based methods like radiography or radioscopy is the capability to display the internal structure in 3D and the resulting possibility to perform the analysis slice by slice with respect to failures, porosity, inclusion, fiber orientation, etc. e.g. [2,6–8]. However, so far high operating expenses due to long analysis and reconstruction times display major disadvantages of lab based XCT systems. This becomes highly crucial if plenty of test objects need to be tested, or the prize per unit is lower or comparable than the measurement and analysis costs. In this context, pearl testing represents a good example, where from individual test objects of unclear origin and value to plenty of test objects, need to be tested. Today the vast majority of pearls on the market are cultured ones from pearl farms. In 2010 China already produced 20 tons of cultured saltwater pearls from the Akoya oyster and 1500 tons of freshwater cultured pearls from different mussels. Australia is the major producer of South Sea pearls worldwide with ten tons per year, while Tahiti provides 16 tons of black pearls per year [9]. Due to the big variety on the pearl market the distinction

* Corresponding author.

E-mail address: roland.brunner@mcl.at (R. Brunner).

<http://dx.doi.org/10.1016/j.csndt.2016.08.002>

2214-6571/© 2016 The Author(s). Published by Elsevier Ltd. This is an open access article under the CC BY-NC-ND license (<http://creativecommons.org/licenses/by-nc-nd/4.0/>).

Table 1

Summarizes the relevant parameters used for the XCT scans of the pearl necklace.

FOD [mm]	FDD [mm]	Voxel size [μm]	No. of images	Scanning time [min]	Reconstruction time [min]	Voltage [kV]
86	300	28.6	2400	20	4	55

between natural and cultured pearls becomes more and more demanding. Today's equipment for pearl testing comprises a great diversity of methods, as described by [10] and references therein. Two NDT methods widely used to characterize the interior of the pearls are X-ray radiography and X-ray radioscopy, applying X-ray sensitive films and digital X-ray detectors respectively. X-ray micro-computed tomography (μ -XCT) represents a more recent method to characterize pearls [11]. In contrast to X-ray radiography and X-ray radioscopy, long measurement and reconstruction times prevented μ -XCT from a wide use in NDT. However, X-ray radiography and radioscopy have some disadvantages, especially when it is necessary to interpret small or complex internal features like thin layers, fissures, small cavities or enclosed material. Even if a pearl is radiographed from different directions, the images give incomplete two-dimensional information about the pearl. Therefore radiography, although consuming less analysis time, may result in misleading interpretations [11]. Therefore, the application of fast characterization of pearls by using XCT would be highly preferable for accurate NDT.

In this case study we use a so-called nano-focus XCT system (nf-XCT) to map the internal structure of a pearl necklace which is composed of about 200 pearls. We show for the first time that the pearls in the necklace can be classified according to their internal features within one scan. Furthermore, we demonstrate that the performed inspection time of about 24 minutes is far lower than those reported previously for single pearls and give comparable 3D image data quality for the inspection (e.g. [11]). The study shows that XCT becomes highly competitive in comparison to other established fast X-ray methods like X-ray radiography or X-ray radioscopy.

2. Method

In this study we use a nanotom *m* (GE Measurement and Control Solutions) lab system, operating a nano-focus X-ray tube™ with a maximum acceleration voltage of 180 kV and maximum X-ray current of 880 μ A. The used XTC system is based on a cone beam configuration where the sample is rotated around 360° within the X-ray and located between the X-ray tube and detector indicated by the focal object distance (FOD) and the focal detector distance (FDD), respectively (Table 1). The minimum focal spot size is about 800 nm. However, the focal spot size of this X-ray tube can be optimized according to the resolution needed for the particular task. Here, an optimization for a voxel size of 28.6 μ m was performed (Table 1). The detector installed in the nanotom *m* provides 3052 \times 2400 pixels, with 100 μ m per pixel which gives an overall detector area of about 300 \times 240 mm. The flat panel detector provides a high dynamic range of greater than 10000:1 and low noise which enables low exposure times [12]. This large area and dynamic range gives room for the possibility to crop the used detector area however maintaining still sufficient image quality. The exposure time for one single image and overall number of projections taken for a scan was 500 ms. Such an nf-XCT system is capable to realize (1) a voxel size of about 400 nm [13], or (2) as demonstrated in this paper, allows fast 3D inspection as shown for the pearl necklace with an image quality comparable to previous studies obtained for single pearls. The scanning and reconstruction time including the specific sample related parameters are summarized in Table 1. The used parameters were optimized to provide information regarding characteristic features necessary to distinguish between natural and cultured pearls with shortest possible inspection times. The inspection time is thereby defined as the sum of scanning and reconstruction time. A resume concerning characteristic features of natural and cultured pearls is briefly given in e.g. in [11]. The characteristic of natural pearls is mainly defined by an onion-like growing structure of thick calcium carbonate and thin less dense conchiolin layers. Cultured pearls, in contrast to natural pearls like fresh water non-beaded pearls contain small cavity structures in their centre. Several test scans for the optimization of image quality (amount of grey values, pixels and reduced artefacts) have been performed in advance on individual pearls and pearl necklaces. These found parameters give a good basis for any further fast pearl inspection. For the reconstruction [14] of the 3D volume a commercial software package is applied (datos 2 rec). The software is also used to reduce artefacts like beam hardening. For short reconstruction times a commercially available desktop workstation with 192 GB RAM and an external graphic interface unit with five additional GPUs is used.

3. Results and discussion

In the following, we show that the nf-XCT setup is highly suitable to characterize not only individual pearls but also to analyse a number of pearls at once, as necessary for multiple pearl testing e.g. for a necklace. Fig. 1 shows the measurement setup where the pearl necklace composed of about 200 individual pearls is fixed straightforwardly with pins on a foam block. It has to be taken into account that the pearl necklace has to be positioned in the path of the X-rays in such a way that the overall material thickness is low enough to be permeated by the low-energy X-rays (Table 1).

In Fig. 2 the nf-XCT 3D data of an exemplary pearl necklace is depicted. The necklace exists of small pearls. Each shows a diameter between 2–2.5 mm. Clearly the drill holes can be seen. In the following discussion we focus on three pearls within the necklace as indicated by I, II and III. Fig. 3 shows slice images from three directions of pearl I and its vicinity. Fig. 3(a)

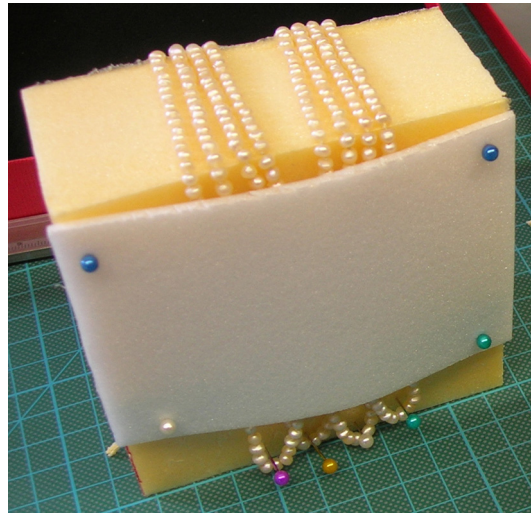


Fig. 1. Measurement setup showing the prepared sample ready for the XCT measurement. The pearls are fixed with pins on a foam block.

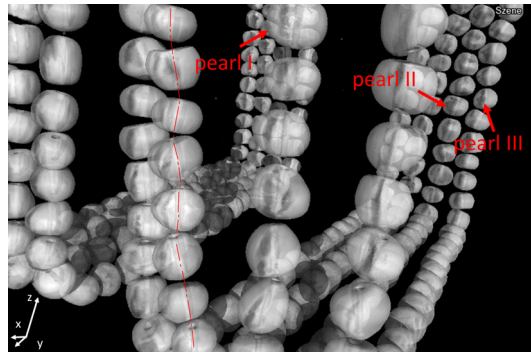


Fig. 2. 3D reconstructed pearl necklace. The labels "I", "II" and "III" highlight the pearls mainly discussed in the following images. The direction of the drill holes is presented by the dashed line through the centre of the drill holes.

shows a slice image through the centre of two representative pearls in the x - y plane. The pearl labeled with I shows a drilling hole in the centre (lowest grey value: black). Around the drilling hole mainly two regions can be distinguished. The region closer to the centre with a lateral extension of about 1.5 mm shows in comparison to the region between 1.5 to about 2 mm much darker grey values. This difference in the grey values may arise from the appearance of various calcium carbonate phases e.g. calcite, vaterite or amorphous calcium carbonate. The different phases have different densities. The higher the density is, the lighter the observed grey value will be. In addition between the calcium carbonate phases, fissure like structures in darkest grey are shown. The latter correlates to a horny protein called conchiolin which serves as a binder within the pearl. In Fig. 3(b) and (c) the slice image in the z - y and z - x plane are shown, respectively. Again one can see the fine conchiolin-rich region around the centre region of the calcium carbonate matrix. The spherical almost symmetrical extent of the inner region suggesting the formation of a nucleus is supported by the three slice images.

Fig. 4 gives an example of a pearl with a nearly concentric onion like growing structure consisting of the carbonate matrix and thin conchiolin layers in between. Within the projections the drilling holes remain again as a black area. Fig. 4(a) shows the slice image in the x - y -plane. The thicker carbonate layers from pearl II are shown as light grey whereas the thinner conchiolin layers are indicated by a darker grey. The average thickness of the carbonate layers (thicker layer: lighter grey values) is about 0.78 ± 0.12 mm. In the vicinity an additional example of a pearl, which is labeled as pearl III is presented. The pearl shows a similar behavior as pearl I in Fig. 3(a). Again different calcium carbonate phases with different densities represented as different grey values are shown. The slice images of pearl II shown in Fig. 4(b) and (c) give additional information regarding the workmanship of the pearl necklace. In both slice images it can be seen that according to the characteristic of the thin conchiolin layer close to the surface, a machining of the pearl surface like polishing took place.

The XCT images prove that the quality loss due to the larger scanning area in comparison to single pearl scans is negligible. The 3D image data provides enough information regarding the classification of each individual pearl within the

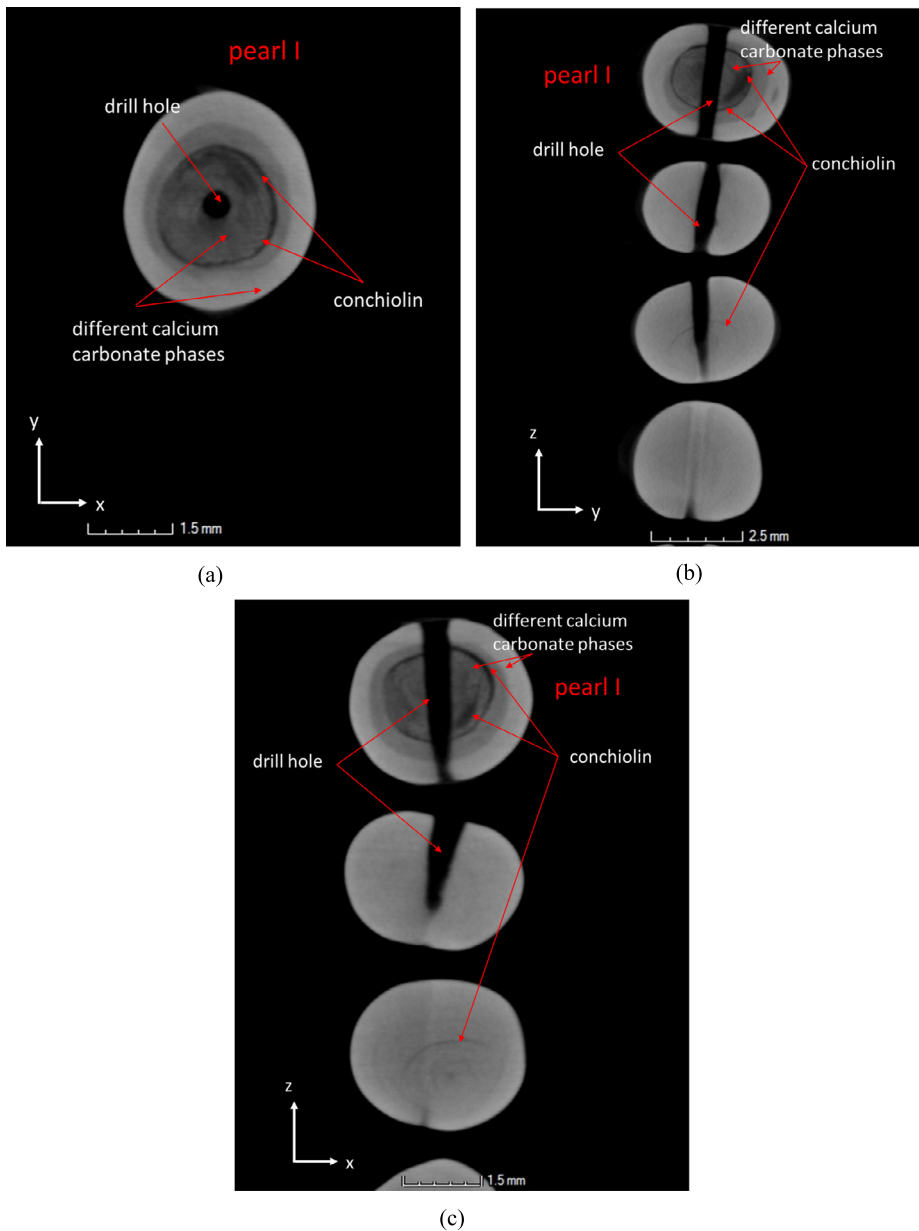


Fig. 3. Shows an example of a presumably natural pearl labeled with "I". The central area shows a spherical region with darker grey values (lower densities) than the outer area (higher density). (a) Slice image in the x-y plane. The drill hole (black), different calcium carbonate phases (different densities: lighter to darker grey) and conchiolin layer (lower density: darkest grey) are labeled in the image. (b) Slice image in the z-x-plane. (c) Slice image in the z-y-plane.

necklace. A distinction between cultured and natural pearls using the discussed settings is still possible (Figs. 3, 4). According to the presented investigations of the internal features of the pearls, especially due appearance of the typical features for natural pearls, we conclude that the presented pearls (Fig. 3, 4) are natural.

The X-ray radioscopic data, as shown in Fig. 5 gives no information regarding the growth structure or internal features of the pearls. Therefore, no accurate classification regarding cultured and natural pearls within the pearl necklace can be given with this method.

4. Conclusion

It has been shown that the nf-XCT scans presented in this work have been trimmed to decrease inspection times as much as possible, while still providing reliable information regarding the distinction of natural and cultured pearls within the

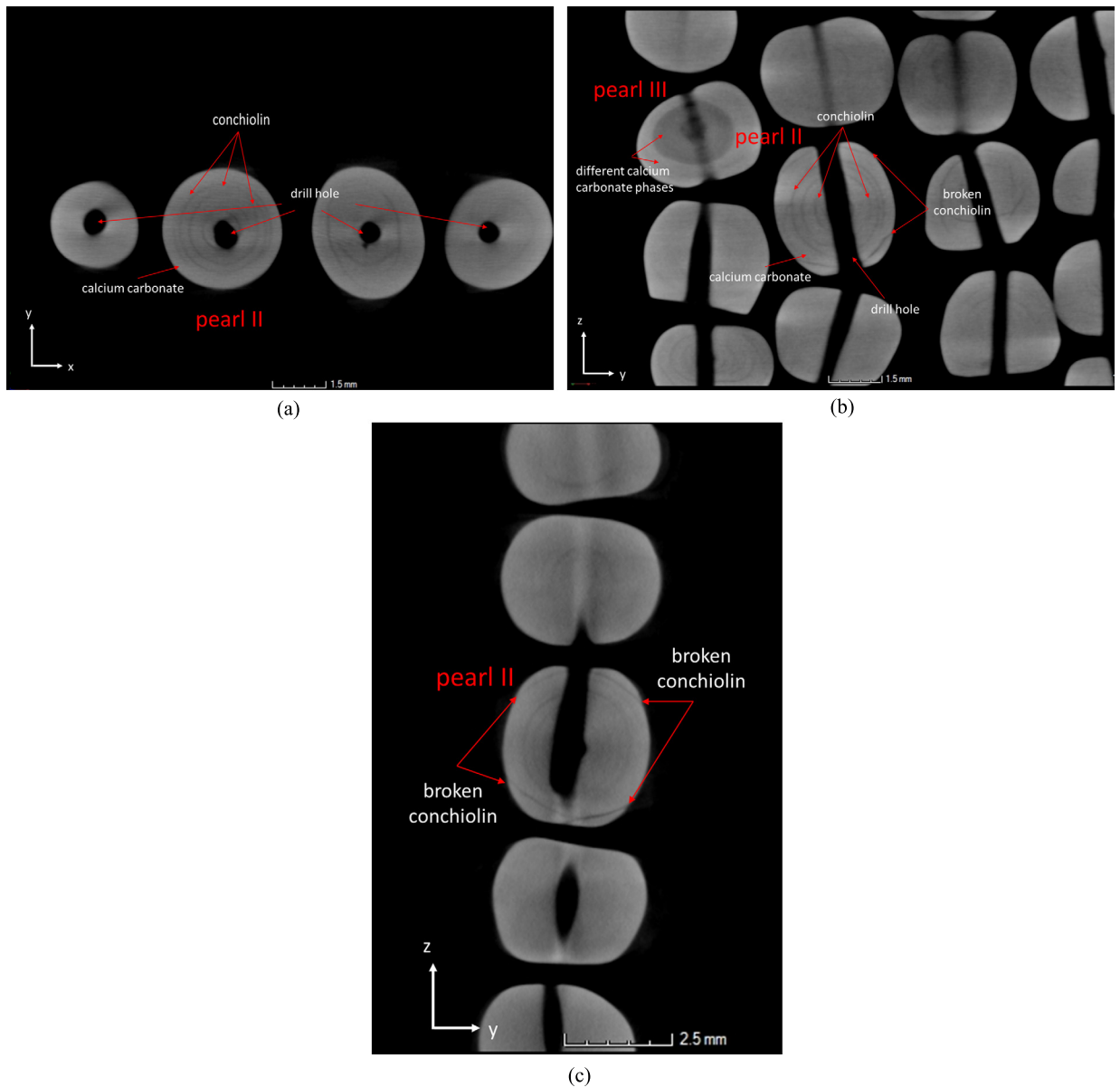


Fig. 4. An example of another presumably natural pearl with typical concentric structures of the nacre layers, labeled with “II”, is given. (a) Slice image in the x - y plane. The onion like growth structure is indicated by the fissures (low intensity: darker grey) around the centre of the pearl. (b) Slice image in the z - x -plane. The thin conchiolin lines (darker grey) are broken at the surface. This suggests the application of a processing step like polishing which have been used to artificially reshape the pearl. (c) Slice image in the z - y -plane. Also the broken conchiolin layers are shown at the surface.

necklace. The nano-focus setup including a temperature stabilized X-ray tube, target, high contrast detector, user experience and discussed settings, allow the possibility to perform measurements of several pearls with one scan with an inspection time of 24 min. It implies the possibility to scan and reconstruct individual pearls within less than ten minutes while maintaining sufficient data quality. Further, the work demonstrates that the presented approach is competitive regarding measurement time scales to NDT methods like X-ray radiography as well as X-ray radioscopy. However, with the clear advantage that three-dimensional information is derived by using computed tomography. The formation of the nucleus-like structure within pearl I is still under discussion and will need further investigation. We would like to point out that the presented approach, regarding the decrease of scanning time, is not limited to the field of pearl testing. Such scans can also be performed with samples from other fields used in material science, microelectronics, etc. However we omit, that the application of such fast scans well below one hour is strongly dependent on the composition of the sample and will need additional sample specific studies.

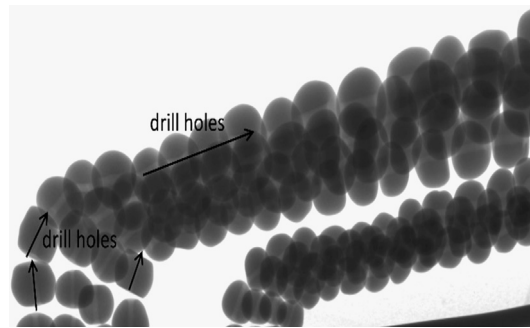


Fig. 5. Radioscopy image of the pearl. The drill holes are labeled. No characteristic information about the interior and characteristic of the pearls can be extracted. A distinction between natural and cultured pearls is not possible.

Acknowledgements

The authors acknowledge KommR Prof. Elfriede Schwarzer, from E. Swietly Peony, pearl dealer in Vienna since 1953, for reliable information and numberless different and typical pearl samples. Our further thanks go to Mag. Astrid Fialka-Herics, head of the Department Jewels and Jewelry at auction house Dorotheum in Vienna for valuable collaboration. Financial support by the Austrian Federal Government (in particular from Bundesministerium für Verkehr, Innovation und Technologie and Bundesministerium für Wissenschaft, Forschung und Wirtschaft) represented by Österreichische Forschungsförderungsgesellschaft mbH and the Styrian and the Tyrolean Provincial Government, represented by Steirische Wirtschaftsförderungsgesellschaft mbH and Standortagentur Tirol, within the framework of the COMET Funding Programme (P.No. 837900) is gratefully acknowledged.

References

- [1] du Plessis A, le Roux SG, Els J, Booysen G, Blaine DC. Application of microCT to the no-destructive testing of an manufactured titanium component. *Case Stud Nondistruc Test Evaluat* 2015;4:1–7.
- [2] Yadav SD, Rosc J, Sartory B, Brunner R, Sonderegger B, Sommitsch C, et al. Investigation of pre-existing pores in creep loaded 9Cr steel'. In: *Proc. conf. 2nd int. Congress on '3D materials science'*. The Minerals, Metals & Materials Society; 2014. p. 85–90.
- [3] Boussein ML, Boyd SK, Christensen BA, Gulberg RE, Jepsen KJ, Müller R. Guidelines for assessment of bone microstructure in rodents using micro-computed tomography. *J Bone Miner Res* 2010;25(7):1468–86.
- [4] Genant HK, Block JE, Steiger P, Glueer CC, Smith R. Quantitative computed tomography in assessment of osteoporosis. *Semin Nucl Med* 1987;17:316–33.
- [5] Rosc J, Hammer H, Kraker E, Pfeiler-Deutschmann M, Parteder G, Hlina W, et al. Reliability assessment of contact wires in LED-devices using. In: *Situ X-ray computed tomography and thermo-mechanical simulations, IEEE conference: electronic system-integration technology conference*. 2014. p. 1–6.
- [6] Cason M, Estrada R. Application of X-ray MicroCT for non-destructive failure analysis and package construction characterization. In: *18th IEEE international symposium on the physical and failure analysis of integrated circuits*. 2011. p. 1–6.
- [7] Moore MJ, Jabbar E, Ritman EL, Lu L, Currier BL, Windbank AJ, et al. Quantitative analysis of interconnectivity of porous biodegradable scaffolds with micro computed tomography. *J Biomed Mater Res, Part A* 2004;1:258–67.
- [8] Cosmi F, Bernasconi A, Sodini N. Phase contrast micro-tomography and morphological analysis of a short carbon fibre reinforced polyamide. *Compos Sci Technol* 2011;71(1):23.
- [9] Cartier LE, Ali SH. China's Pearl industry: an indicator of ecological stress. <http://www.greenconduct.com/blog/2013/01/23/chinas-pearl-industry-an-indicator-of-ecological-stress/#sthash.u011iW7W.dpuf>, 2013.
- [10] Krzemnicki MS, Hajdas I. Age determination of pearls: a new approach for pearl testing and identification. In: *Proc. on the 21st international radiocarbon conference, Radiocarbon*, vol. 55(2/3). 2012. p. 1801–9.
- [11] Krzemnicki MS, Friess SD, Chalus P, Hänni HA, Karamelas S. X-ray computed microtomography: distinguishing natural pearls from beaded and non-beaded cultured pearls. *G&G* 2010;46(2):128–34. <http://dx.doi.org/10.5741/GEMS.46.2.128>.
- [12] Brunke O, Neuser E, Suppes A. High resolution industrial CT systems: advances and comparison with synchrotron-based CT. In: *Proc. international symposium on digital radioscopy and computed tomography tu.3.2*. 2011. p. 1–9.
- [13] Rosc J, Brunner R. 2015. personal communication.
- [14] Feldkamp LA, Davis LC, Kress JW. Practical cone-beam algorithm. *J Opt Soc Am A* 1984;1:612–9. <http://dx.doi.org/10.1364/JOSAA.1.000612>.